

Super-localized orthogonal decomposition for high-frequency Helmholtz problems

Philip Freese, Moritz Hauck, Daniel Peterseim

Angaben zur Veröffentlichung / Publication details:

Freese, Philip, Moritz Hauck, and Daniel Peterseim. 2024. "Super-localized orthogonal decomposition for high-frequency Helmholtz problems." *SIAM Journal on Scientific Computing* 46 (4): A2377–97. <https://doi.org/10.1137/21M1465950>.



SUPER-LOCALIZED ORTHOGONAL DECOMPOSITION FOR HIGH-FREQUENCY HELMHOLTZ PROBLEMS*

PHILIP FREESE[†], MORITZ HAUCK[‡], AND DANIEL PETERSEIM[§]

Abstract. We propose a novel variant of the Localized Orthogonal Decomposition (LOD) method for time-harmonic scattering problems of Helmholtz type with high wavenumber κ . On a coarse mesh of width H , the proposed method identifies local finite element source terms that yield rapidly decaying responses under the solution operator. They can be constructed to high accuracy from independent local snapshot solutions on patches of width ℓH and are used as problem-adapted basis functions in the method. In contrast to the classical LOD and other state-of-the-art multiscale methods, two- and three-dimensional numerical computations show that the localization error decays super-exponentially as the oversampling parameter ℓ is increased. This suggests that optimal convergence is observed under the substantially relaxed oversampling condition $\ell \gtrsim (\log \frac{\kappa}{H})^{(d-1)/d}$ with d denoting the spatial dimension. Numerical experiments demonstrate the significantly improved offline and online performance of the method also in the case of heterogeneous media and perfectly matched layers.

Key words. Helmholtz equation, high-frequency, heterogeneous media, numerical homogenization, multiscale method, super-localization

MSC codes. 65N12, 65N15, 65N30, 35J05

DOI. 10.1137/21M1465950

1. Introduction. This paper studies the numerical solution of time-harmonic acoustic scattering problems that can be modeled by the Helmholtz equation. The standard variational formulation of the Helmholtz problem is an indefinite and non-hermitian problem and, especially for large wavenumbers κ , its numerical solution is a challenging task. Due to the highly oscillatory nature of the analytical solution and the κ -dependent pollution effect [2], classical polynomial-based finite element methods need to meet very restrictive conditions on the mesh size H of the underlying mesh. Typically, these conditions are much stronger than the minimal requirement $H\kappa \lesssim 1$ from approximation theory needed for the approximation of an oscillatory function.

In the literature, there have been many attempts to tackle this issue. We highlight two classes of methods that are theoretically able to suppress the pollution effect, namely hp -finite elements and multiscale methods. The strategy of hp -finite elements [44, 45, 43] is to couple the polynomial degree p of the approximation space to κ in a logarithmic way. Then, the quasi-optimality of the numerical approximation can be ensured under the resolution condition $H\kappa \lesssim p$.

*Submitted to the journal's Numerical Algorithms for Scientific Computing section December 22, 2021; accepted for publication (in revised form) March 20, 2024; published electronically July 18, 2024.

<https://doi.org/10.1137/21M1465950>

Funding: This work was part of a project that received funding from the European Research Council ERC under the European Union's Horizon 2020 research and innovation program (grant agreement 865751). The work of the first author was partially supported by the Deutsche Forschungsgemeinschaft (DFG, German Research Foundation) Project-ID 258734477 - SFB 1173.

[†]Chair Computational Mathematics, Institute of Mathematics, Hamburg University of Technology, Hamburg, Germany (philip.freese@tuhh.de).

[‡]Department of Mathematics, University of Augsburg, Universitätsstr. 12a, 86159, Augsburg, Germany (moritz.hauck@uni-a.de).

[§]Department of Mathematics & Centre for Advanced Analytics and Predictive Sciences (CAAPS), University of Augsburg, Universitätsstr. 12a, 86159, Augsburg, Germany (daniel.peterseim@uni-a.de).

Multiscale methods, in contrast, use problem-adapted ansatz spaces, which are constructed by solving multiple mutually independent local problems. An effective approach for constructing such problem-adapted ansatz spaces is the Localized Orthogonal Decomposition (LOD). The LOD was originally introduced as a numerical homogenization method for elliptic diffusion problems with arbitrary rough coefficients [40, 35, 41] and was later generalized to Helmholtz problems [29, 49, 12, 50, 51, 32]. Its basis functions are computed by solving local subspace correction problems on element patches of size ℓH with ℓ denoting the oversampling parameter of the method. Faithful numerical approximations to the Helmholtz problem are obtained under the resolution condition $H\kappa \lesssim 1$ and the oversampling condition $\ell \gtrsim \log \kappa$. With their higher degree of adaptivity with respect to the problem, multiscale methods and especially the LOD are intrinsically able to handle heterogeneous coefficients and singularities in the analytical solution. Those scenarios are not easily treated in methods with universal shape functions such as *hp*-finite elements.

Certainly, there exist many other numerical methods for the Helmholtz problem that have not been mentioned yet. Widely known is the class of Trefftz methods [57, 17, 55, 36], which use, on each mesh element, functions that are locally solutions of the Helmholtz equation as test and trial functions (e.g., plane waves, generalized harmonic polynomials). Moreover, also other multiscale methods such as the multiscale spectral generalized finite element method [18], the (generalized) multiscale finite element method [25, 26, 16], the heterogeneous multiscale method [47], and the multiscale hybrid-mixed method [15] have been successfully applied to the Helmholtz problem. We emphasize that LOD-based methods use one (problem-adapted) basis function per mesh entity and achieve their accuracy by mesh refinement, while generalized finite element methods (such as [18, 16]) use a fixed partition of the domain into subdomains and achieve their accuracy by increasing the number of functions per subdomain. For a recent work that combines both concepts, see [24].

The LOD implicitly computes its problem-adapted ansatz spaces as approximation to the space given by the application of the solution operator to some (coarse) classical finite element space; see [1]. This connection has recently been exploited in [33] to develop a conceptually new LOD multiscale method for the elliptic multiscale problem. It identifies local source terms in the coarse finite element space that yield rapidly decaying (in some cases even local) responses under the solution operator. This rapid decay makes it possible to approximate the global responses by localized counterparts, which are solutions to problems on element patches of size ℓH in the coarse grid. These localized responses are then used as problem-adapted basis functions. The error caused by this approximation is henceforth referred to as localization error. For the elliptic multiscale problem, the localization errors of the novel multiscale method decay super-exponentially as ℓ is increased. This is a substantial improvement compared to the existing localization strategies [40, 35, 38, 37, 8] with exponentially decaying localization errors.

This paper aims to show that the novel localization strategy is not limited to the elliptic model problem but, just like the LOD, can be generalized to a large variety of problem classes beyond elliptic homogenization problems. As a proof of concept, this paper generalizes the novel localization strategy [33] to a class of indefinite and non-hermitian problems represented by the Helmholtz problem in the high-frequency regime. Under a stability assumption on the basis of the method and the resolution condition $H\kappa\ell \lesssim 1$ (in practice also $H\kappa \lesssim 1$ seems to be sufficient), a κ -explicit stability and error analysis of the proposed multiscale method is presented; see Theorems 5.2 and 5.3. The stability and error estimates are explicit in quantities that

are proportional to the smallest singular value of some patch-local coarse-scale operators. Two- and three-dimensional numerical experiments clearly demonstrate a super-exponential decay of the singular values as ℓ is increased, although a rigorous mathematical proof is still open. Given the super-exponential decay of the singular values, the oversampling condition needed for the stability and optimal order convergence of the method is $\ell \gtrsim (\log \frac{\kappa}{H})^{(d-1)/d}$ with d denoting the spatial dimension. This condition is a major improvement over the corresponding condition for the LOD, which is $\ell \gtrsim \log \frac{\kappa}{H}$.

This relaxed oversampling condition is of great practical importance as, especially for large κ , it enables significant computational savings compared to the LOD. First and foremost, the relaxed oversampling condition allows for smaller patch problems, which considerably reduces the offline computational costs. Moreover, also the online computational costs are lower due to the improved locality of the basis functions, which implies a sparser coarse system matrix.

For the sake of simplicity, our analysis covers only Helmholtz problems in homogeneous media. Nevertheless, in the spirit of [12, 51], the method naturally extends to the case of heterogeneous media, which is demonstrated numerically in section 6. In addition, this paper addresses the issue of physically meaningful boundary conditions. Although widely used and convenient for mathematical theory, the impedance boundary condition as an approximation of the Dirichlet-to-Neumann map on some artificial boundary yields significant errors, especially for large κ ; see [27]. Similarly, as in [14] for the LOD, we demonstrate that the proposed multiscale method is naturally and easily combined with perfectly matched layers (PML) [5, 19, 6], which are known to be an effective and efficient way to eliminate spurious reflections at the artificial boundary.

The structure of this paper is as follows. Section 2 briefly introduces the model problem and states some important analytical results. In section 3, we present a prototypical multiscale method with optimal κ -independent convergence rates. Using the novel localization approach presented in section 4, the method is then turned into a practically feasible scheme in section 5. Finally, section 6 illustrates the performance of the proposed method in numerical experiments. We show that the approach is also applicable to heterogeneous media and can be easily combined with the PML.

2. Model problem. Let us consider the Helmholtz equation with homogeneous impedance boundary conditions on a bounded Lipschitz polytope $\Omega \subset \mathbb{R}^d$, $d = 1, 2, 3$, which is assumed to be scaled to unit size. Explicitly, Ω is an interval, a polygon, and a polyhedron, in dimensions $d = 1, 2, 3$, respectively. Given a right-hand side $f \in L^2(\Omega)$, we seek $u: \Omega \rightarrow \mathbb{C}$ being the solution of

$$(2.1) \quad \begin{aligned} -\Delta u - \kappa^2 u &= f && \text{in } \Omega, \\ \nabla u \cdot n - i\kappa u &= 0 && \text{on } \partial\Omega, \end{aligned}$$

with $\kappa > 0$ denoting the wavenumber, i the imaginary unit, and n the outward unit normal vector. The weak formulation of (2.1) is based on the sesquilinear form $a: \mathcal{V} \times \mathcal{V} \rightarrow \mathbb{C}$ which acts on the solution space $\mathcal{V} := H^1(\Omega)$ (the space of complex-valued square-integrable functions on Ω with square-integrable weak derivative) and is defined as

$$a(u, v) := (\nabla u, \nabla v)_{L^2(\Omega)} - \kappa^2(u, v)_{L^2(\Omega)} - i\kappa(u, v)_{L^2(\partial\Omega)}.$$

From a theoretical perspective it is possible to phrase the Helmholtz problem in a different variational setting where the sesquilinear form is coercive; cf. [46]. For practical

reasons we stick to the classical indefinite sesquilinear form. The inner products of the spaces $L^2(\Omega)$ and $L^2(\partial\Omega)$ (the spaces of complex-valued square-integrable functions on Ω and $\partial\Omega$, respectively) are denoted by $(\cdot, \cdot)_{L^2(\Omega)}$ and $(\cdot, \cdot)_{L^2(\partial\Omega)}$, respectively.

As usual in the Helmholtz context, the solution space \mathcal{V} is endowed with the following κ -dependent norm:

$$\|u\|_{\mathcal{V}}^2 := \|\nabla u\|_{L^2(\Omega)}^2 + \kappa^2 \|u\|_{L^2(\Omega)}^2.$$

With respect to this norm, the sesquilinear form a is continuous, i.e., there is a κ -independent constant $C_a > 0$ such that

$$|a(u, v)| \leq C_a \|u\|_{\mathcal{V}} \|v\|_{\mathcal{V}}.$$

For a given $f \in L^2(\Omega)$, Fredholm theory [42] shows that there exists a unique weak solution $u \in \mathcal{V}$ to the weak formulation of (2.1), such that, for all $v \in \mathcal{V}$,

$$(2.2) \quad a(u, v) = (f, v)_{L^2(\Omega)}$$

satisfying

$$(2.3) \quad \|u\|_{\mathcal{V}} \leq C_{\text{st}}(\kappa) \|f\|_{L^2(\Omega)}$$

with a κ -dependent constant $C_{\text{st}}(\kappa) > 0$.

For the geometric configuration in this work, i.e., bounded Lipschitz domain and pure impedance boundary conditions, it can be shown that C_{st} depends polynomially on κ . Specifically, [23] shows $C_{\text{st}} = \mathcal{O}(\kappa^{5/2})$ while in [54] even $C_{\text{st}} = \mathcal{O}(\kappa^{3/4})$ is obtained. For the case where Ω is convex or smooth and star shaped with respect to a ball, it is proved in [7, 20, 42] that $C_{\text{st}} = \mathcal{O}(1)$. A discussion of the general Lipschitz case is found in [54] and that $C_{\text{st}} = \mathcal{O}(1)$ for general C^∞ domains is proved in [3]. It should be noted that for more general boundary conditions and non-convex geometries, trapping scenarios can arise with C_{st} growing at least exponentially in κ ; see [7] for an example.

An immediate consequence of (2.3) is the inf-sup stability of a

$$(2.4) \quad 0 < \alpha(\kappa) \leq \inf_{u \in \mathcal{V}} \sup_{v \in \mathcal{V}} \frac{\Re a(u, v)}{\|u\|_{\mathcal{V}} \|v\|_{\mathcal{V}}} = \inf_{u \in \mathcal{V}} \sup_{v \in \mathcal{V}} \frac{\Re a(u, v)}{\|u\|_{\mathcal{V}} \|v\|_{\mathcal{V}}}$$

with $\alpha(\kappa) = (2C_{\text{st}}(\kappa)\kappa)^{-1}$ and $\Re z$ denoting the real part of the complex number $z \in \mathbb{C}$.

We will refer to $\mathcal{L}: L^2(\Omega) \rightarrow \mathcal{V}$ as the solution operator of the Helmholtz problem, mapping $f \in L^2(\Omega)$ to the unique solution $u \in \mathcal{V}$ of the weak formulation (2.2). For $z \in \mathbb{C}$ we denote with \bar{z} the complex conjugate. The solution operator to the adjoint Helmholtz problem, i.e., $a(u, v)$ in (2.2) is substituted by $\overline{a(v, u)}$, is denoted by \mathcal{L}^* . As shown in [45, Lemma 3.1], for $f \in L^2(\Omega)$ the solution operators \mathcal{L} and \mathcal{L}^* are connected by the relation

$$(2.5) \quad \mathcal{L}^* f = \overline{\mathcal{L} \bar{f}}.$$

Remark 2.1 (heterogeneous media, scatterers, boundary conditions). The construction of our method is easily extended to more complicated scenarios of heterogeneous materials, scattering problems, and, for instance, mixtures of Dirichlet, Neumann, and Robin boundary conditions. It shall be mentioned that the well-posedness of Helmholtz problems in heterogeneous media is a delicate issue; see [53, 30, 31] for some recent results.

3. Prototypical multiscale method. This section introduces a prototypical multiscale method which has convergence properties independent of the wavenumber. Its trial and test spaces are obtained by applying the (adjoint) solution operator to right-hand sides in classical finite element spaces. Such methods are only considered for theoretical purposes, as in general, global problems need to be solved for computing the method's basis functions.

Let us introduce the possibly coarse, conforming mesh \mathcal{T}_H consisting of closed simplicial or quadrilateral (convex) elements with a diameter at most $H > 0$. Henceforth, we assume that \mathcal{T}_H is quasi-uniform in the sense of [9, Definition 4.4.13]. Denoting with $\mathbb{P}_0(\mathcal{T}_H)$ the space of \mathcal{T}_H -piecewise constant functions, we define $\Pi_H: L^2(\Omega) \rightarrow \mathbb{P}_0(\mathcal{T}_H)$ as the L^2 -orthogonal projection onto $\mathbb{P}_0(\mathcal{T}_H)$. Recall that, for all $T \in \mathcal{T}_H$, it satisfies the following local stability and approximation properties (see [48, 4]):

$$(3.1) \quad \begin{aligned} \|\Pi_H v\|_{L^2(T)} &\leq \|v\|_{L^2(T)} && \text{for all } v \in L^2(T), \\ \|v - \Pi_H v\|_{L^2(T)} &\leq \pi^{-1} H \|\nabla v\|_{L^2(T)} && \text{for all } v \in H^1(T). \end{aligned}$$

We introduce a prototypical problem-adapted Petrov–Galerkin method which is based on the trial and test spaces

$$\mathcal{V}_H := \text{span}\{\mathcal{L}\mathbf{1}_T \mid T \in \mathcal{T}_H\}, \quad \mathcal{V}_H^* := \text{span}\{\mathcal{L}^*\mathbf{1}_T \mid T \in \mathcal{T}_H\},$$

where $\mathbf{1}_T$ denotes the characteristic function of an element $T \in \mathcal{T}_H$. The prototypical multiscale method seeks $u_H \in \mathcal{V}_H$ such that, for all $v_H \in \mathcal{V}_H^*$,

$$(3.2) \quad a(u_H, v_H) = (f, v_H)_{L^2(\Omega)}.$$

The following necessary assumption ensures that the coarse mesh \mathcal{T}_H is able to resolve oscillatory Helmholtz solutions; see Lemma 3.2 below.

Assumption 3.1 (resolution condition). Suppose that the mesh size of \mathcal{T}_H satisfies

$$H\kappa \leq \frac{\pi}{\sqrt{2}}.$$

Under this assumption, the well-posedness and the κ -independent approximation properties of the prototypical Petrov–Galerkin method can be proved.

LEMMA 3.2 (stability and κ -independent approximation). *If Assumption 3.1 is fulfilled, then the sesquilinear form a is inf–sup stable with regard to the trial space \mathcal{V}_H and the test space \mathcal{V}_H^* , i.e., there exists $C_{\text{id}} > 0$ independent of κ and H such that*

$$C_{\text{id}} \inf_{u_H \in \mathcal{V}_H} \sup_{v_H \in \mathcal{V}_H^*} \frac{\Re a(u_H, v_H)}{\|u_H\|_{\mathcal{V}} \|v_H\|_{\mathcal{V}}} \geq \alpha(\kappa) > 0.$$

Here, α denotes the inf–sup constant of the continuous problem (2.2).

Moreover, there exists $C_{\text{er}} > 0$ independent of κ and H such that, for all right-hand sides $f \in H^s(\Omega)$ with $s \in [0, 1]$, the unique solution u_H of the Petrov–Galerkin method (3.2) satisfies the κ -independent error bound

$$\frac{\pi}{2} \|u - u_H\|_{\mathcal{V}} \leq H \|f - \Pi_H f\|_{L^2(\Omega)} \leq C_{\text{er}} H^{1+s} |f|_{H^s(\Omega)},$$

where $|\cdot|_{H^s(\Omega)}$ denotes the H^s -seminorm with $|\cdot|_{H^0(\Omega)} := \|\cdot\|_{L^2(\Omega)}$.

Proof. For a proof, see, e.g., [1, Theorem 3.9 and Example 3.10a] and [32, Lemma 4.6 and 4.7]. \square

4. Localization strategy. The canonical basis functions $\{\mathcal{L}\mathbf{1}_T \mid T \in \mathcal{T}_H\}$ and $\{\mathcal{L}^*\mathbf{1}_T \mid T \in \mathcal{T}_H\}$ of the problem-adapted trial and test spaces \mathcal{V}_H and \mathcal{V}_H^* , respectively, are non-local and have a slow (algebraic) decay. For a practically feasible variant of method (3.2), localized bases have to be identified. Recently, in [33], a novel localization approach was introduced for the elliptic model problem which has superior localization properties compared to other state-of-the-art approaches [40, 35, 38, 37, 8]. This section extends this novel localization approach to a class of indefinite non-hermitian problems, using the Helmholtz problem as an example. In contrast to [32], the target regime of the proposed method is the high-frequency case where the oscillatory behavior of the solution is just resolved by the coarse mesh \mathcal{T}_H . For this regime, the multiresolution approach in [32] is not applicable.

By relation (2.5), it suffices to analyze the localization of the trial space \mathcal{V}_H , as a localized basis of the test space can then be obtained without further computation. The idea of the localization strategy is to identify local \mathcal{T}_H -piecewise constant source terms that yield rapidly decaying (or even local) responses under the solution operator \mathcal{L} of the Helmholtz problem.

Our localization is based on (local) patches, given as neighborhoods of mesh elements, in the coarse mesh \mathcal{T}_H . The first order element patch $\mathbf{N}(S) = \mathbf{N}^1(S)$ of a union of elements $S \subset \Omega$ is given by

$$\mathbf{N}^1(S) := \bigcup \{T \in \mathcal{T}_H \mid T \cap S \neq \emptyset\}.$$

The ℓ th order patch $\mathbf{N}^\ell(T)$, $\ell = 2, 3, 4, \dots$, of T is then recursively given by

$$\mathbf{N}^\ell(T) := \mathbf{N}^1(\mathbf{N}^{\ell-1}(T));$$

see Figure 1 for a schematic illustration.

For the subsequent derivation, we fix an oversampling parameter $\ell \in \mathbb{N}$ and denote, for arbitrary $T \in \mathcal{T}_H$, the ℓ th order patch of T by $\omega := \mathbf{N}^\ell(T)$. Let ℓ be chosen such that no patch coincides with the domain Ω . On the patch ω , we define the space $\mathcal{V}_\omega := \{v|_\omega \mid v \in \mathcal{V}\}$, i.e., the restriction of \mathcal{V} to the patch ω . Furthermore, let $\mathcal{T}_{H,\omega}$ denote the submesh of \mathcal{T}_H with elements in ω and let $\Pi_{H,\omega}: L^2(\omega) \rightarrow \mathbb{P}_0(\mathcal{T}_{H,\omega})$ denote the $L^2(\omega)$ -orthogonal projection onto $\mathbb{P}_0(\mathcal{T}_{H,\omega})$.

The novel localization strategy requires the solution of local patch problems with Dirichlet and impedance boundary conditions prescribed on $\Gamma := \partial\omega \setminus \partial\Omega$ and $\partial\omega \cap \partial\Omega$, respectively. For proving the well-posedness of such problems, we need the Friedrich inequality (see, e.g., [9, 52]), which states the existence of a constant $C_F > 0$ such that, for all $v \in \mathcal{V}_{\omega,\Gamma} := \{v \in \mathcal{V}_\omega \mid v|_\Gamma = 0\}$,

$$(4.1) \quad \|v\|_{L^2(\omega)} \leq C_F H \ell \|\nabla v\|_{L^2(\omega)}.$$

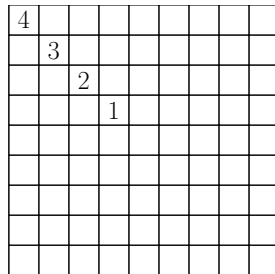


FIG. 1. Illustration of an ℓ th order patch for $\ell = 1, \dots, 4$ with grayscale indicating the order.

Henceforth, we suppose that C_F is independent of the parameters H and ℓ ; see also the following remark.

Remark 4.1 (Friedrich's constant). For example, provided that all patches can be obtained as an affine transformation of a bounded number of reference domains, one can prove that C_F is independent of H and ℓ ; see also [56, Corollary A.15]. This is true, for example, if Ω has a rather simple geometry (e.g., a d -dimensional brick) and \mathcal{T}_H is a Cartesian mesh. Note that the condition that C_F is independent of H and ℓ also appears for the multiscale method introduced in [18, Lemma 3.12]. We emphasize that for the general setting, however, the dependence of C_F on the parameters H and ℓ cannot be found explicitly.

The following assumption poses a stronger condition on the smallness of the mesh size than Assumption 3.1.

Assumption 4.2 (resolution condition revisited). Suppose that the mesh size of \mathcal{T}_H satisfies

$$H\kappa\ell \leq \frac{1}{C_F\sqrt{2}}.$$

In the numerical experiments in section 6 we do not account for this stronger condition but rather choose our discretization parameters based on the weaker condition Assumption 3.1. Even for this weaker condition, which is the same as for the LOD [50, 32], the patch problems seem to be stable to solve.

The following lemma states the coercivity of the form $a_\omega: \mathcal{V}_\omega \times \mathcal{V}_\omega \rightarrow \mathbb{C}$,

$$a_\omega(u, v) := (\nabla u, \nabla v)_{L^2(\omega)} - \kappa^2(u, v)_{L^2(\omega)} - i\kappa(u, v)_{L^2(\partial\Omega \cap \partial\omega)},$$

with respect to the norm $\|\cdot\|_{\mathcal{V}_\omega}^2 := \|\nabla \cdot\|_{L^2(\omega)}^2 + \kappa^2\|\cdot\|_{L^2(\omega)}^2$.

LEMMA 4.3 (coercivity of a_ω). *If Assumption 4.2 is fulfilled, it holds, for all $v \in \mathcal{V}_{\omega, \Gamma}$, that*

$$\Re a_\omega(v, v) \geq \frac{1}{3}\|v\|_{\mathcal{V}_\omega}^2.$$

Proof. For all $v \in \mathcal{V}_{\omega, \Gamma}$, we obtain using Friedrich's inequality (4.1) and Assumption 4.2

$$\Re a_\omega(v, v) = \|\nabla v\|_{L^2(\omega)}^2 - \kappa^2\|v\|_{L^2(\omega)}^2 \geq (1 - C_F^2 H^2 \ell^2 \kappa^2) \|\nabla v\|_{L^2(\omega)}^2 \geq \frac{1}{2} \|\nabla v\|_{L^2(\omega)}^2.$$

The coercivity follows when utilizing that

$$\|v\|_{\mathcal{V}_\omega}^2 = \|\nabla v\|_{L^2(\omega)}^2 + \kappa^2\|v\|_{L^2(\omega)}^2 \leq (1 + C_F^2 \kappa^2 H^2 \ell^2) \|\nabla v\|_{L^2(\omega)}^2 \leq \frac{3}{2} \|\nabla v\|_{L^2(\omega)}^2$$

for all $v \in \mathcal{V}_{\omega, \Gamma}$. □

We aim to identify (almost) local basis functions $\varphi = \varphi_{T, \ell} \in \mathcal{V}_H$ associated with the element $T \in \mathcal{T}_H$. For (generally complex) coefficients $(c_K)_{K \in \mathcal{T}_{H, \omega}}$ that need to be determined afterwards, the construction of these basis functions follows the ansatz

$$\varphi = \mathcal{L}g \quad \text{with} \quad g = g_{T, \ell} := \sum_{K \in \mathcal{T}_{H, \omega}} c_K \mathbf{1}_K.$$

The Galerkin projection of such a given φ onto the local subspace $\mathcal{V}_{\omega,\Gamma}$ defines a localized approximation $\varphi^{\text{loc}} = \varphi_{T,\ell}^{\text{loc}} \in \mathcal{V}_{\omega,\Gamma}$, which satisfies, for all $v \in \mathcal{V}_{\omega,\Gamma}$,

$$(4.2) \quad a_{\omega}(\varphi^{\text{loc}}, v) = (g, v)_{L^2(\omega)}.$$

Due to the coercivity of a_{ω} (Lemma 4.3) and the Lax–Milgram lemma, φ^{loc} is well defined. In general, the local function φ^{loc} is a poor approximation of the possibly global function φ . However, there exist non-trivial choices of g that yield highly accurate approximations in the \mathcal{V} -norm. The following discussion requires a brief reminder on traces of \mathcal{V}_{ω} -functions; see [39] for details. We denote the trace operator restricted to $\Gamma \subset \partial\omega$ by

$$\gamma_0 = \gamma_{0,\omega}: \mathcal{V}_{\omega} \rightarrow H^{1/2}(\Gamma)$$

and abbreviate its range by $X := H^{1/2}(\Gamma)$. For given $t \in X$, we define the Helmholtz-harmonic extension γ_0^{-1} , which is a continuous right-inverse of γ_0 . To be precise, the extension operator $\gamma_0^{-1}t \in \mathcal{V}_{\omega}$ satisfies $\gamma_0\gamma_0^{-1}t = t$ and is Helmholtz-harmonic; precisely, we define $\gamma_0^{-1}t$ by

$$(4.3) \quad a_{\omega}(v, \gamma_0^{-1}t) = 0$$

for all $v \in \mathcal{V}_{\omega,\Gamma}$. Note that well-posedness is again ensured by the coercivity of a_{ω} ; see Lemma 4.3. Now we state our main observation, which establishes a criterion for the choice of g ensuring the smallness of the localization error. Using the properties of the trace and Helmholtz-harmonic extension operators, we obtain from (4.2) and (4.3), utilizing $v - \gamma_0^{-1}\gamma_0v \in \mathcal{V}_{\omega,\Gamma}$, that

$$a(\varphi^{\text{loc}}, v) = a_{\omega}(\varphi^{\text{loc}}, v) = a_{\omega}(\varphi^{\text{loc}}, v - \gamma_0^{-1}\gamma_0v) = (g, v - \gamma_0^{-1}\gamma_0v).$$

Together with the definition of φ this yields

$$(4.4) \quad a(\varphi - \varphi^{\text{loc}}, v) = (g, v)_{L^2(\omega)} - a_{\omega}(\varphi^{\text{loc}}, v) = (g, \gamma_0^{-1}\gamma_0v)_{L^2(\omega)}$$

for all $v \in \mathcal{V}$. This may equivalently be rephrased using the smallness of the normal derivative of φ^{loc} on Γ . Hence, by (4.4), the inf–sup stability of the continuous problem (2.4), a small localization error is equivalent to choosing g (almost) L^2 -orthogonal to the space

$$(4.5) \quad Y := \gamma_0^{-1}X \subset \mathcal{V}_{\omega}$$

of Helmholtz-harmonic functions on ω . An optimal realization of g can hence be achieved by the singular value decomposition (SVD) of the operator $\Pi_{H,\omega}|_Y$, which has at most rank $M := \#\mathcal{T}_{H,\omega}$. More precisely, the SVD is given by

$$(4.6) \quad \Pi_{H,\omega}|_Y v = \sum_{m=1}^M \sigma_m(v, w_m)_{\mathcal{V}_{\omega}} g_m$$

with the singular values $\sigma_1 \geq \dots \geq \sigma_M \geq 0$, the $L^2(\omega)$ -orthonormal piecewise constant left singular vectors g_1, \dots, g_M , and the \mathcal{V}_{ω} -orthonormal right singular vectors w_1, \dots, w_M . Here, we denote by $(\cdot, \cdot)_{\mathcal{V}_{\omega}} := (\nabla \cdot, \nabla \cdot)_{L^2(\omega)} + \kappa^2(\cdot, \cdot)_{L^2(\omega)}$ the weighted

inner product on \mathcal{V}_ω . We choose g as the (L^2 -normalized) right singular vector corresponding to the smallest singular value, i.e., $g := g_M$. To measure the L^2 -orthogonality of g on Y , we define the quantity σ_T as

$$(4.7) \quad \sigma_T(\kappa, H, \ell) := \sigma_M = \sup_{v \in Y} \frac{(g, v)_{L^2(\omega)}}{\|v\|_{\mathcal{V}_\omega}}.$$

For comments on the numerical realization of the SVD, we refer the reader to section 6.

We conjecture that σ_T decays super-exponentially in ℓ , which is subsequently justified with two- and three-dimensional numerical experiments.

CONJECTURE 4.4 (super-exponential decay). *The quantity σ_T decays super-exponentially in ℓ , i.e., there exists a constant $C_{\text{sd}}(\kappa, H, \ell) > 0$ depending polynomially on κ, H^{-1} , and ℓ , but being independent of T and a constant $C > 0$ independent of κ, H, ℓ , and T such that*

$$(4.8) \quad \sigma_T(\kappa, H, \ell) \leq C_{\text{sd}}(\kappa, H, \ell) \exp\left(-C\ell^{\frac{d}{d-1}}\right).$$

Remark 4.5 (the case $d = 1$). For one spatial dimension, the space Y of Helmholtz-harmonic functions is at most two-dimensional. Thus, for $\ell \geq 1$, g can indeed be chosen L^2 -orthogonal on Y , i.e., the basis is in fact local. This locality is in line with our conjecture interpreting $\frac{d}{d-1}$ as infinity. Figure 2 shows the local SLOD basis functions and the ideal (non-localized) LOD basis functions from [32] corresponding to an interior element and an element at the boundary. It shall be noted that the imaginary part of the LOD basis function corresponding to the interior element is very small and thus not visible. For the respective SLOD basis function, the imaginary part is zero as it does not touch the boundary.

Next, we provide numerical experiments for dimensions $d = 2, 3$ demonstrating the super-exponential decay of the singular values of the operator $\Pi_{H,\omega}|_Y$ and thus

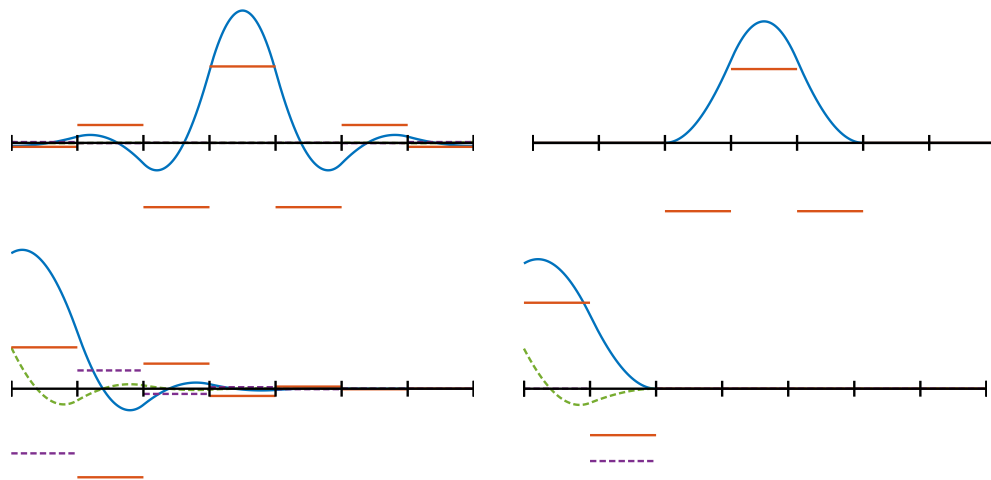


FIG. 2. Global ideal LOD basis (left) and local SLOD basis for $\ell = 1$ (right) with their corresponding L^2 -normalized right-hand sides g in one space dimension for an interior element (top) and an element at the boundary (bottom). The real (resp., imaginary) parts are depicted using solid (resp., dashed) lines.

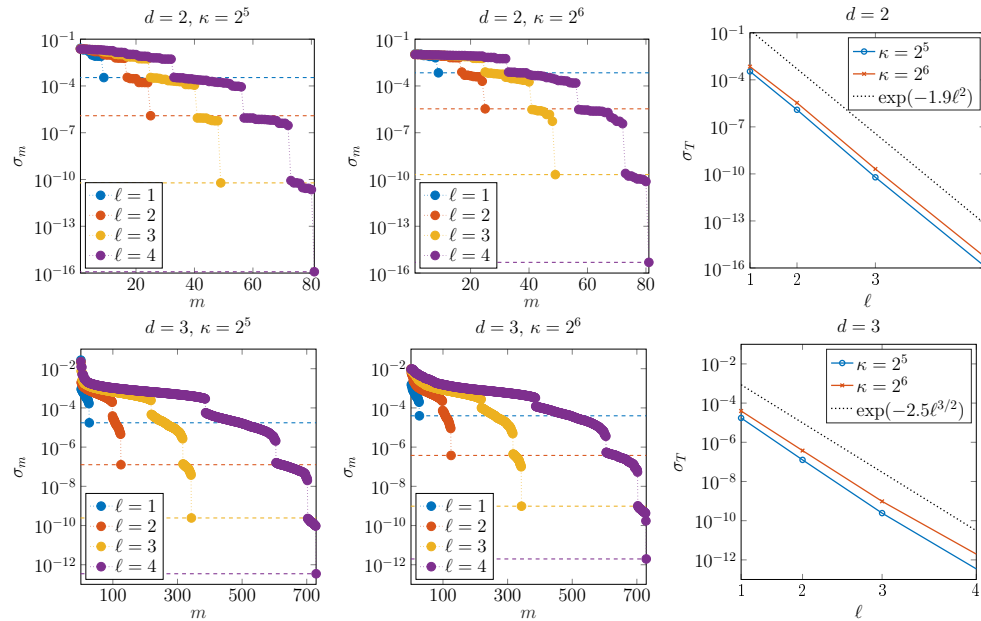


FIG. 3. Singular values σ_m of the operator $\Pi_{H,\omega}|_Y$ in descending order for several oversampling parameters for spatial dimensions $d = 2$ (top) and $d = 3$ (bottom) and for $\kappa = 2^5$ (left) and $\kappa = 2^6$ (middle). The smallest singular values relevant for the definition of σ_T in (4.7) are indicated with dashed horizontal lines. Plot of σ_T in dependence of ℓ (right). The scaling of the x-axis is such that a super-exponentially decaying curve (cf. (4.8)) appears to be an affine function.

justifying Conjecture 4.4. We choose an element T of a fixed Cartesian mesh \mathcal{T}_H far from the boundary and consider the patches $\omega = N^\ell(T)$, $\ell = 1, \dots, 4$; see section 6 for the exact setup of the numerical experiment. Figure 3 (left and middle) depicts the singular values of the operator $\Pi_{H,\omega}|_Y$ in a semilogarithmic plot, and Figure 3 (right) plots the resulting σ_T as a function of ℓ .

One observes that (in a semilogarithmic plot) the distance between the smallest singular values increases by a factor of 2 ($d = 2$) and $3/2$ ($d = 3$) from one ℓ to the next larger one. Note that for $\ell = 4$ the jump is smaller than expected, due to the finite precision arithmetic of the computer. The increased distances correspond to the super-exponential decay of the smallest singular value. The super-exponential decay can be seen even more clearly in Figure 3 (right), where only the smallest singular values are plotted. We point out that for all ℓ the smallest singular value is well separated. Therefore, the choice of g as the right singular vector corresponding to this singular value (cf. (4.7)) is meaningful. For patches touching the boundary, one observes a decay behavior similar to that in Figure 3.

Using techniques from LOD theory [41, 1], one can rigorously derive a pessimistic bound for σ_T . This pessimistic bound shows that the novel localization techniques perform at least as well as state-of-the-art approaches like the LOD.

LEMMA 4.6 (pessimistic exponential decay). *The quantity $\sigma_T(\kappa, H, \ell)$ decays at least exponentially in ℓ , i.e., there exist constants $C, C' > 0$ independent of κ, H, ℓ , and T such that*

$$\sigma_T(\kappa, H, \ell) \leq C' \max\{1, H^{-1}\kappa^{-1}\} \exp(-C\ell).$$

Proof. This result can be proved using techniques from LOD theory and can be obtained by straightforward modifications of the proof of [33, Lemma 6.4]. \square

5. Super-localized multiscale method. Using the novel localization strategy of the previous section, we turn the prototypical multiscale method (3.2) into a feasible scheme. For a fixed oversampling parameter ℓ , we define the ansatz space of the localized method as the span of the localized basis functions $\varphi_{T,\ell}^{\text{loc}}$ defined in (4.2), i.e.,

$$\mathcal{V}_{H,\ell} := \text{span}\{\varphi_{T,\ell}^{\text{loc}} \mid T \in \mathcal{T}_H\}, \quad \mathcal{V}_{H,\ell}^* := \text{span}\{\varphi_{T,\ell}^{\text{loc},*} \mid T \in \mathcal{T}_H\}.$$

The localized method then calculates the Petrov–Galerkin approximation with trial space $\mathcal{V}_{H,\ell}$ and test space $\mathcal{V}_{H,\ell}^*$, i.e., it seeks $u_{H,\ell} \in \mathcal{V}_{H,\ell}$ such that, for all $v_{H,\ell} \in \mathcal{V}_{H,\ell}^*$,

$$(5.1) \quad a(u_{H,\ell}, v_{H,\ell}) = (f, v_{H,\ell})_{L^2(\Omega)}.$$

A minimal requirement for the stability and convergence of the Galerkin method (5.1) is that $\{g_{T,\ell} \mid T \in \mathcal{T}_H\}$ spans $\mathbb{P}_0(\mathcal{T}_H)$ in a stable way. Numerically, this can be ensured as outlined in [33, Appendix B]. For the subsequent numerical analysis, we make the following assumption.

Assumption 5.1 (riesz stability). The set $\{g_{T,\ell} \mid T \in \mathcal{T}_H\}$ is a Riesz basis of $\mathbb{P}_0(\mathcal{T}_H)$, i.e., there exists a constant $C_{\text{rb}}(\kappa, H, \ell) > 0$ depending only polynomially on κ, H^{-1} , and ℓ such that, for all $(c_T)_{T \in \mathcal{T}_H}$, it holds that

$$C_{\text{rb}}^{-1}(\kappa, H, \ell) \sum_{T \in \mathcal{T}_H} |c_T|^2 \leq \left\| \sum_{T \in \mathcal{T}_H} c_T g_{T,\ell} \right\|_{L^2(\Omega)}^2 \leq C_{\text{rb}}(\kappa, H, \ell) \sum_{T \in \mathcal{T}_H} |c_T|^2.$$

In what follows, we investigate the inf–sup stability and the convergence properties of the novel super-localized multiscale method. The respective estimates are explicit in the quantity

$$\sigma(\kappa, H, \ell) := \max_{T \in \mathcal{T}_H} \sigma_T(\kappa, H, \ell).$$

The following theorem shows that the novel method is inf–sup stable under a condition on the oversampling parameter ℓ .

THEOREM 5.2 (stability). *Let Assumptions 4.2 and 5.1 be satisfied and let ℓ be chosen such that*

$$(5.2) \quad \begin{aligned} \varepsilon(\kappa, H, \ell) &:= \alpha^{-1}(\kappa)(1 + 3C_a)C_a C_{\text{ol}} C_b H^{-1} \ell^{d/2} C_{\text{rb}}^{1/2}(\kappa, H, \ell) \sigma(\kappa, H, \ell) \\ &\leq \min \left\{ \frac{1}{2}, \frac{\alpha(\kappa)}{27C_a C_{\text{id}}} \right\} \end{aligned}$$

with α denoting the inf–sup constant of the continuous problem (2.4) and $C_{\text{ol}}, C_b > 0$ depending only on mesh properties of \mathcal{T}_H (quasi-uniformity). Then, the localized method (5.1) is inf–sup stable, i.e., there exists a constant $C_{\text{lo}} > 0$ independent of κ, H , and ℓ such that

$$C_{\text{lo}} \inf_{u_{H,\ell} \in \mathcal{V}_{H,\ell}} \sup_{v_{H,\ell} \in \mathcal{V}_{H,\ell}^*} \frac{\Re a(u_{H,\ell}, v_{H,\ell})}{\|u_{H,\ell}\|_{\mathcal{V}} \|v_{H,\ell}\|_{\mathcal{V}}} \geq \alpha(\kappa).$$

Proof. Let us consider the following bijective mapping between \mathcal{V}_H and $\mathcal{V}_{H,\ell}$:

$$\iota: \mathcal{V}_H \rightarrow \mathcal{V}_{H,\ell}, u_H := \sum_{T \in \mathcal{T}_H} c_T \varphi_{T,\ell} \mapsto \sum_{T \in \mathcal{T}_H} c_T \varphi_{T,\ell}^{\text{loc}} =: u_{H,\ell}.$$

First, we show the continuity of ι . For arbitrary $u_{H,\ell} \in \mathcal{V}_{H,\ell}$, the triangle inequality yields

$$\|u_{H,\ell}\|_{\mathcal{V}} \leq \|u_H\|_{\mathcal{V}} + \|u_H - u_{H,\ell}\|_{\mathcal{V}}.$$

Using the inf-sup stability of the continuous problem (2.4) combined with (4.4), we obtain for the second term that there exists $v \in \mathcal{V}$ with $\|v\|_{\mathcal{V}} = 1$ such that

$$\begin{aligned} \alpha(\kappa) \|u_H - u_{H,\ell}\|_{\mathcal{V}} &\leq \Re a(u_H - u_{H,\ell}, v) \leq \left| \sum_{T \in \mathcal{T}_H} c_T (g_{T,\ell}, \gamma_0^{-1} \gamma_0 v)_{L^2(\omega)} \right| \\ &\leq \sum_{T \in \mathcal{T}_H} \sigma_T(\kappa, H, \ell) |c_T| \|\gamma_0^{-1} \gamma_0 v\|_{\mathcal{V}_\omega}, \end{aligned}$$

where we used (4.7) in the last inequality. From Lemma 4.3 we deduce the estimate

$$(5.3) \quad \|\gamma_0^{-1} \gamma_0 v\|_{\mathcal{V}_\omega} \leq (1 + 3C_a) \|v\|_{\mathcal{V}_\omega},$$

which holds independently of the patch ω . Using that $\|v\|_{\mathcal{V}} = 1$, the finite overlap of the patches yields

$$(5.4) \quad \sum_{T \in \mathcal{T}_H} \|v\|_{\mathcal{V}_\omega}^2 \leq \sum_{T \in \mathcal{T}_H} C_{\text{ol}}^2 \ell^d \|v\|_{\mathcal{V}_T}^2 = C_{\text{ol}}^2 \ell^d,$$

where $C_{\text{ol}}^2 \ell^d$ bounds the number of patches containing a fixed mesh element.

We denote with $\tilde{\Pi}_H: L^2(\Omega) \rightarrow \mathcal{V}$ the operator which maps L^2 -functions to their conforming counterparts with the same element averages, which are constructed as linear combination of element-local bubble functions (see, e.g., [10, 58]). Such an operator satisfies for some $C_b > 0$ the estimate $\|\tilde{\Pi}_H v\|_{\mathcal{V}} \leq C_b H^{-1} \|v\|_{L^2(\Omega)}$ for all $v \in \mathcal{V}$. Using this, we obtain for any $p \in \mathbb{P}(\mathcal{T}_H)$ that

$$(5.5) \quad \|p\|_{L^2(\Omega)} = \sup_{v \in \mathcal{V}} \frac{(p, v)_{L^2(\Omega)}}{\|v\|_{L^2(\Omega)}} \leq C_b H^{-1} \sup_{v \in \mathcal{V}} \frac{(p, \tilde{\Pi}_H v)}{\|\tilde{\Pi}_H v\|_{\mathcal{V}}} \leq C_b H^{-1} \|p\|_{\mathcal{V}^*}.$$

From the Cauchy-Schwarz inequality, (5.3)–(5.5), and Assumption 5.1, we get

$$\begin{aligned} \alpha(\kappa) \|u_H - u_{H,\ell}\|_{\mathcal{V}} &\leq (1 + 3C_a) C_{\text{ol}} \ell^{d/2} \sigma(\kappa, H, \ell) \sqrt{\sum_{T \in \mathcal{T}_H} |c_T|^2} \\ &\leq (1 + 3C_a) C_{\text{ol}} \ell^{d/2} C_{\text{rb}}^{1/2}(\kappa, H, \ell) \sigma(\kappa, H, \ell) \left\| \sum_{T \in \mathcal{T}_H} c_T g_{T,\ell} \right\|_{L^2(\Omega)} \\ &\leq (1 + 3C_a) C_a C_b C_{\text{ol}} H^{-1} \ell^{d/2} C_{\text{rb}}^{1/2}(\kappa, H, \ell) \sigma(\kappa, H, \ell) \|u_H\|_{\mathcal{V}} \end{aligned}$$

and thus, using (5.2), $\|u_{H,\ell}\|_{\mathcal{V}} \leq \frac{3}{2} \|u_H\|_{\mathcal{V}}$, i.e., the continuity of ι . Similarly, one can show $\|u_H\|_{\mathcal{V}} \leq 2 \|u_{H,\ell}\|_{\mathcal{V}}$, i.e., the continuity of ι^{-1} . The same estimates can analogously be shown for

$$\iota^*: \mathcal{V}_H^* \rightarrow \mathcal{V}_{H,\ell}^*, v_H := \sum_{T \in \mathcal{T}_H} c_T \varphi_{T,\ell}^* \mapsto \sum_{T \in \mathcal{T}_H} c_T \varphi_{T,\ell}^{\text{loc},*} =: v_{H,\ell}.$$

Second, we show the inf-sup stability of the localized problem using the inf-sup stability of the continuous problem (2.4). We consider a fixed but arbitrary $u_{H,\ell} \in \mathcal{V}_{H,\ell}$ and define $u_H := \iota^{-1}u_{H,\ell} \in \mathcal{V}_H$. Furthermore, we set $v_{H,\ell} := \iota^*v_H \in \mathcal{V}_{H,\ell}^*$, where $v_H \in \mathcal{V}_H^*$ is chosen such that

$$\Re a(u_H, v_H) \geq \frac{\alpha(\kappa)}{C_{\text{id}}} \|u_H\|_{\mathcal{V}} \|v_H\|_{\mathcal{V}};$$

cf. Lemma 3.2. Algebraic manipulations and elementary estimates yield

$$\Re a(u_{H,\ell}, v_{H,\ell}) \geq \Re a(u_H, v_H) - |a(u_{H,\ell} - u_H, v_H)| - |a(u_{H,\ell}, v_{H,\ell} - v_H)|.$$

We estimate the terms on the right-hand side separately. For the first term, we obtain using the continuity of ι and ι^* that

$$\Re a(u_H, v_H) \geq \frac{\alpha(\kappa)}{C_{\text{id}}} \|u_H\|_{\mathcal{V}} \|v_H\|_{\mathcal{V}} \geq \frac{\alpha(\kappa)}{3C_{\text{id}}} \|u_{H,\ell}\|_{\mathcal{V}} \|v_{H,\ell}\|_{\mathcal{V}}.$$

For the second term, one obtains using (5.2)

$$|a(u_{H,\ell} - u_H, v_H)| \leq C_a \|u_{H,\ell} - u_H\|_{\mathcal{V}} \|v_H\|_{\mathcal{V}} \leq \frac{\alpha(\kappa)}{9C_{\text{id}}} \|u_{H,\ell}\|_{\mathcal{V}} \|v_{H,\ell}\|_{\mathcal{V}}.$$

The third term can be estimated analogously. Absorbing the second and the third terms in the first, the inf-sup stability of the localized method follows. \square

Provided that the stability constant C_{st} from (2.3) depends polynomially on κ (see the discussion in section 2), and using Conjecture 4.4, the oversampling condition (5.2) can be rewritten as

$$(5.6) \quad \ell \gtrsim (\log \frac{\kappa}{H})^{(d-1)/d}.$$

As seen in the following theorem, the asymptotically same condition also guarantees an optimal order of convergence. In both cases, this is a substantial improvement compared to the oversampling conditions for the LOD, which are $\ell \gtrsim \log \kappa$ for stability and $\ell \gtrsim \log \frac{\kappa}{H}$ for an optimal order of convergence. It shall be noted that the κ -dependence in the above oversampling conditions can be eliminated using Assumptions 3.1 and 4.2.

THEOREM 5.3 (convergence). *Let the assumptions from Theorem 5.2 be fulfilled. Then, the solution $u_{H,\ell}$ of the localized Petrov-Galerkin approximation (5.1) satisfies*

$$(5.7) \quad \|u - u_{H,\ell}\|_{\mathcal{V}} \leq \frac{2}{\pi} C_{\text{er}} H^{1+s} \|f\|_{H^s(\Omega)} + \delta(\kappa, H, \ell) \|f\|_{L^2(\Omega)}$$

with

$$\delta(\kappa, H, \ell) = 3(1 + C_a C_{\text{id}} \alpha^{-1}(\kappa)) C_{\text{id}} \kappa^{-1} \alpha^{-1}(\kappa) \varepsilon(\kappa, H, \ell)$$

and $C_{\text{er}}, C_{\text{id}}$ from Lemma 3.2.

Proof. For this proof, we use the notation from the proof of Theorem 5.2. We begin estimating with the triangle inequality

$$\|u - u_{H,\ell}\|_{\mathcal{V}} \leq \|u - u_H\|_{\mathcal{V}} + \|u_H - u_{H,\ell}\|_{\mathcal{V}}.$$

The first term can be estimated using Lemma 3.2. For the second term, we apply Strang's lemma [22, Lemma 2.25] as $u_{H,\ell} \in \mathcal{V}_{H,\ell}$ can be seen as a non-conforming and non-consistent approximation to $u_H \in \mathcal{V}_H$

$$\begin{aligned} \|u_H - u_{H,\ell}\|_{\mathcal{V}} &\leq (1 + C_a C_{\text{id}} \alpha^{-1}(\kappa)) \inf_{w_{H,\ell} \in \mathcal{V}_{H,\ell}} \|u_H - w_{H,\ell}\|_{\mathcal{V}} \\ &\quad + C_{\text{id}} \alpha^{-1}(\kappa) \sup_{v_{H,\ell} \in \mathcal{V}_{H,\ell}^*} \frac{|a(u_H, v_{H,\ell}) - (f, v_{H,\ell})_{L^2(\Omega)}|}{\|v_{H,\ell}\|_{\mathcal{V}}}. \end{aligned}$$

Here, the first term can be estimated, choosing $w_{H,\ell} := \iota u_H$. Using similar arguments as in the proof of Theorem 5.2 yields

$$\|u_H - \iota u_H\|_{\mathcal{V}} \leq \varepsilon(\kappa, H, \ell) \|u_H\|_{\mathcal{V}} \leq C_{\text{id}} \kappa^{-1} \alpha^{-1}(\kappa) \varepsilon(\kappa, H, \ell) \|f\|_{L^2(\Omega)}.$$

For the second term, elementary algebraic manipulations yield, for all $v_H \in \mathcal{V}_H^*$,

$$a(u_H, v_{H,\ell}) - (f, v_{H,\ell})_{L^2(\Omega)} = (f, v_H - v_{H,\ell})_{L^2(\Omega)} - a(u_H, v_H - v_{H,\ell}).$$

Choosing $v_H := \iota^{*-1} v_{H,\ell}$, we obtain

$$\begin{aligned} &|a(u_H, v_{H,\ell}) - (f, v_{H,\ell})_{L^2(\Omega)}| \\ &\leq 2\kappa^{-1} \varepsilon(\kappa, H, \ell) \|f\|_{L^2(\Omega)} \|v_{H,\ell}\|_{\mathcal{V}} + 2C_a C_{\text{id}} \kappa^{-1} \alpha^{-1}(\kappa) \varepsilon(\kappa, H, \ell) \|f\|_{L^2(\Omega)} \|v_{H,\ell}\|_{\mathcal{V}}. \end{aligned}$$

Putting together the estimates finishes the proof. \square

Remark 5.4 (a posteriori bound of the localization error). While the first term on the right-hand side of (5.7) can be controlled a priori, the second term (the localization error) can be bounded a posteriori (the σ_T are computed during the SVD; cf. (4.6)). In addition to the σ_T , the Riesz basis constant C_{rb} needs to be computed (cf. Assumption 5.1), which requires the solution of a global coarse-scale eigenvalue problem. Therefore, possible a posteriori error control strategies are not (quasi-)local but also include coarse-scale global computations.

6. Numerical experiments. In this section, we numerically investigate the proposed multiscale method (hereafter referred to as SLOD) and compare it with the LOD from [32]. All our experiments have been performed using MATLAB and a short version of the code is available as a supplement M146595_SupplementaryMaterials.zip [local/web 4.08KB]. It should be noted that this code is for demonstration purposes only. Thus, the code is not optimized and, for example, does not exploit the structure of the coefficient.

In the following numerical experiments we consider the domain $\Omega := (0, 1)^2$, which is equipped with a coarse Cartesian mesh \mathcal{T}_H of mesh size H (henceforth the mesh size denotes the side length of the elements instead of their diameter). For the discretization of the continuous patch problems (4.2) and (4.3) we use the \mathcal{Q}_1 -finite element method on fine Cartesian meshes of the respective patches with mesh size 2^{-10} . All errors are computed against a \mathcal{Q}_1 -finite element reference solution on the global Cartesian mesh of mesh size 2^{-10} .

The space Y from (4.5) of Helmholtz harmonic functions on the patch $\omega = \mathbf{N}^\ell(T)$ is sampled using $5 \cdot \#\mathcal{T}_{H,\omega}$ samples of random discrete Dirichlet data on $\partial\omega \setminus \partial\Omega$. The random Dirichlet data is generated by linearly interpolating independent and identically distributed (i.i.d.) values (from a uniform distribution) prescribed at the boundary vertices of the fine Cartesian patch mesh lying on $\partial\omega \setminus \partial\Omega$. For more information

on efficient sampling techniques for spaces of harmonic functions, see also [13]. Next, the approximation to Y is used to compute the SVD of the operator $\Pi_{H,\omega}|_Y$. For the numerical realization of the SVD in (4.6), we note that suitable weighting matrices are required to ensure that the right and left singular vectors are \mathcal{V}_ω -orthonormal and $L^2(\omega)$ -orthonormal, respectively. The computation of these weighting matrices requires the inversion and square root of a matrix whose size is proportional to the number of coarse elements in the patch under consideration; cf. [33, Appendix B]. In practice, the effect of the weighting matrices on the choice of SLOD basis functions is hardly noticeable. Therefore, for the numerical experiments in this section, the weighting matrices are omitted in the implementation of the SLOD. It shall also be noted that, for patches ω that are close to the boundary $\partial\Omega$, the choice of g is more involved. Stability for such patches can be ensured by allowing the communication between at most $\mathcal{O}(\ell^d)$ patches. The corresponding algorithm can be found in the supplementary material M146595_SupplementaryMaterials.zip [local/web 4.08KB]; for a discussion of the algorithm, see [33, Appendix B].

Remark 6.1 (computational costs). The computation can be divided into an offline phase, which is independent of the right-hand side, and an online phase, which needs to be repeated if the right-hand side is changed. In the offline phase, the basis functions of the method are precomputed and the coarse stiffness matrix is assembled. Note that (for homogeneous media) it suffices to compute only $\mathcal{O}(\ell^d)$ basis functions, while the remaining ones can be obtained by translation; see [29, section 3]. For a fixed oversampling parameter ℓ , the computational costs for the proposed multiscale method are comparable to those of the LOD (considering the usual LOD implementation described in [21]). However, due to the relaxed oversampling condition (5.6), significantly smaller ℓ 's are sufficient for reaching a prescribed level of accuracy. This shrinks the computational costs, as both the overall number of patch-problems and their size are reduced considerably. For the online phase, the smaller oversampling parameter allows for a sparser system matrix, which, in turn, reduces the computational costs.

6.1. Super-exponential decay of localization error. For this numerical experiment, we consider the right-hand side $f \equiv 1$, as for this choice the error bound in (5.7) holds without the first term, and thus, only the localization error δ remains. Figure 4 shows the relative \mathcal{V} -norm localization errors of our localization approach (referred to as SLOD) and for the stabilized LOD from [32]. The localization errors are plotted for several coarse grids \mathcal{T}_H in dependence of ℓ for $\kappa = 2^5, 2^6$. As a reference, we indicate lines showing the expected rates of decay of the localization errors. Please note the special scaling of the axes, which is chosen such that quadratically exponentially decaying functions appear linear with negative slope.

Figure 4 numerically confirms the super-exponential decay of the localization errors of the proposed multiscale method. The localization error of the LOD decays exponentially; see [35, 40]. This numerical experiment confirms that the SLOD has localization errors several orders of magnitude smaller than the LOD.

6.2. Optimal convergence under mesh refinement. Here, we consider the right-hand side $f(x, y) = \sin(\pi x) \cos(\pi y)$. Figure 5 depicts the relative \mathcal{V} -norm errors for several ℓ in dependence of H for $\kappa = 2^5, 2^6$ in a double-logarithmic plot. As a reference, we indicate a line of slope 2, which is the expected convergence rate in H for right-hand sides $f \in H^1(\Omega)$; see Theorem 5.3.

In Figure 5, one clearly observes convergence of order 2 in H for the SLOD. Note that for the SLOD, the lines corresponding to the oversampling parameters $\ell = 2, 3$

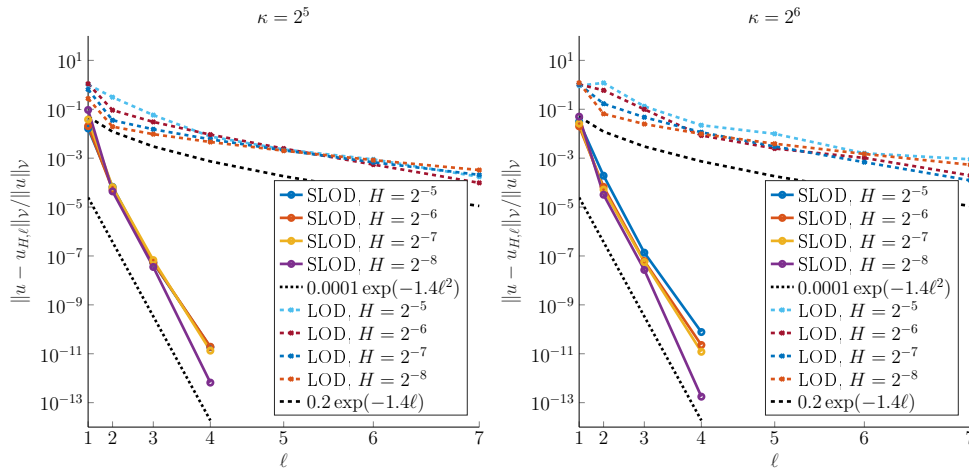


FIG. 4. Localization errors for the SLOD and LOD for several values of H for $\kappa = 2^5$ (left) and $\kappa = 2^6$ (right).

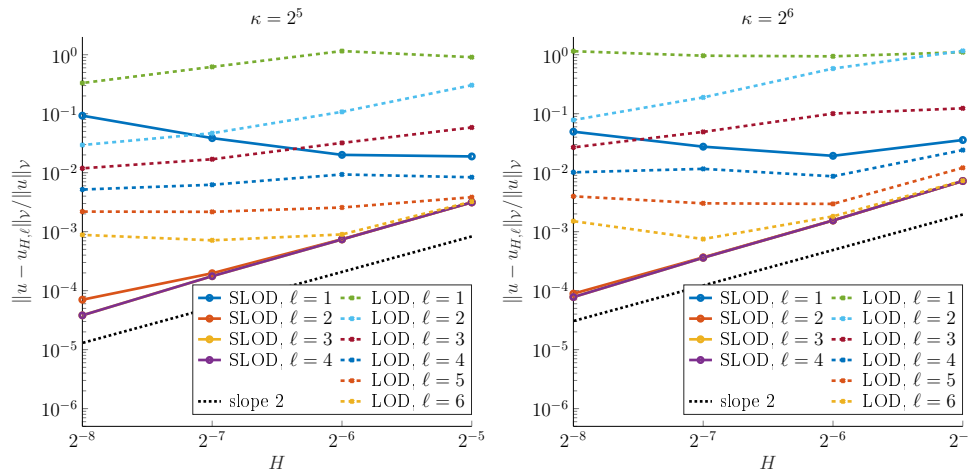


FIG. 5. Convergence plots for the SLOD and LOD for several oversampling parameters ℓ for $\kappa = 2^5$ (left) and $\kappa = 2^6$ (right).

can hardly be distinguished. As, for the LOD, the localization error decays much slower than for the SLOD (see Figure 4), the localization error dominates the overall error. Therefore, for the LOD, one observes the decay of the localization error rather than the desired convergence in H . This numerical experiment demonstrates that, also for relatively high wavenumbers κ , small oversampling parameters such as $\ell = 2, 3$ are sufficient.

6.3. High-contrast heterogeneous media. Here, we demonstrate the application of the SLOD to the heterogeneous Helmholtz equation $-\nabla \cdot (A \nabla u) - \kappa^2 u = f$ with homogeneous impedance boundary conditions. For some parameter $0 < \varepsilon \ll 1$, the coefficient A takes the value ε^2 inside some periodically aligned inclusions of size $\varepsilon/2$ and the value 1 elsewhere; see Figure 6 (left) for a depiction of A . For the choice $\kappa = 9$, a special interplay between the wavenumber and the periodic structure of the inclusions yields a negative-valued effective wavenumber in homogenization theory,

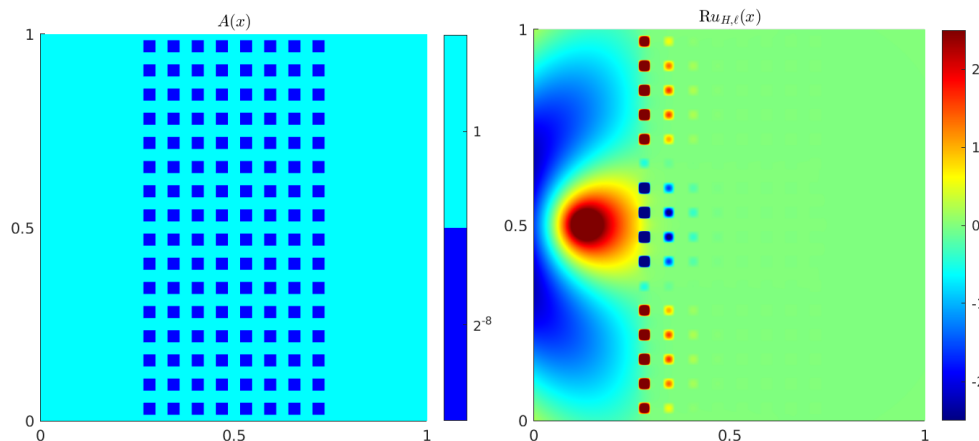


FIG. 6. Heterogeneous coefficient A (left) with $\varepsilon = 2^{-4}$ and real part of the corresponding SLOD solution (right) for $\ell = 2$, $H = 2^{-6}$, and $\kappa = 9$.

which triggers an exponential decay of the modulus of the Helmholtz solution in the bulk domain. This physically interesting effect is caused by Mie resonances in the small inclusions; see [51]. As the right-hand side, we use an approximate point source located at $z = (0.125, 0.5)^T$ that vanishes outside a circle of radius 0.05, i.e.,

$$(6.1) \quad f(x, y) = \begin{cases} 10^4 \cdot \exp\left(\frac{-1}{1 - \frac{(x-z_1)^2 + (y-z_2)^2}{0.05^2}}\right), & (x-z_1)^2 + (y-z_2)^2 < 0.05^2, \\ 0, & \text{else.} \end{cases}$$

Figure 6 (right) depicts the real part of the SLOD solution for $H = 2^{-6}$ and $\ell = 2$. Note that, for the sake of illustration, the color map is truncated to the interval $[-2.5, 2.5]$. The SLOD solution has a relative error of $3.3 \cdot 10^{-3}$ with respect to the weighted norm

$$\|\cdot\|_{\mathcal{V},A}^2 := \|A^{1/2} \nabla \cdot\|_{L^2(\Omega)}^2 + \kappa^2 \|\cdot\|_{L^2(\Omega)}^2.$$

For reaching a similar accuracy on the same coarse mesh, the LOD needs an oversampling parameter of $\ell = 5$, which is a significant difference from $\ell = 2$ for the SLOD.

6.4. Perfectly matched layers (PML). For this numerical experiment, we again consider the point source (6.1), but this time with $z = (0.5, 0.5)^T$.

Our implementation of the perfectly matched layer is similar to [6], but adapted to the multiscale setting. We consider the fixed coarse Cartesian mesh \mathcal{T}_H with $H = 2^{-7}$ and divide the domain Ω into an inner part $\Omega_F := (4H, 1-4H)^2$, the physical domain, and the absorbing layer $\Omega_A := \Omega \setminus \Omega_F$. For this configuration, the absorbing layer has a width of $4H$. The (unbounded) absorbing function in the x -direction is given as

$$\rho_x(x) = \begin{cases} \frac{i}{\kappa} \left(\frac{1}{-x} + \frac{1}{4H} \right), & 0 < x \leq 4H, \\ \frac{i}{\kappa} \left(\frac{1}{1-x} - \frac{1}{4H} \right), & 1-4H \leq x < 1. \end{cases}$$

In the y -direction the absorbing functions are chosen accordingly. As usual for PML, we use homogeneous Dirichlet boundary conditions on $\partial\Omega$. The full PML Helmholtz

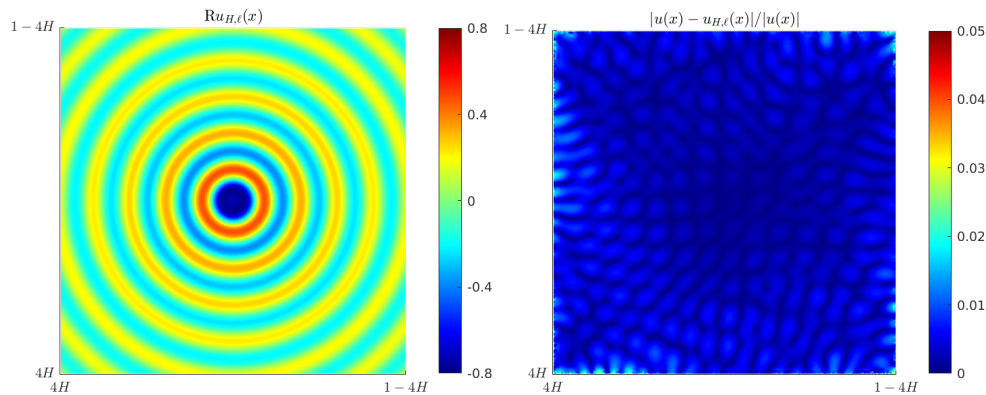


FIG. 7. Real part of SLOD solution with PML (left) and relative error (right) for $\ell = 2$, $H = 2^{-7}$, and $\kappa = 2^6$.

system may be found in [6, section 3]. We apply the SLOD to this PML formulation and truncate the solution to the physical domain Ω_F .

We choose the parameters $\ell = 2$ and $\kappa = 2^6$. Figure 7 shows the real part of the SLOD solution with PML (left) and the relative error computed against the PML reference solution (right). The relative error with respect to $\|\cdot\|_{V_{\Omega_F}}$ is $6.5 \cdot 10^{-3}$.

7. Conclusion. In this paper, we introduced a novel multiscale method for high-frequency Helmholtz problems. It is conceptually similar to the LOD but utilizes a substantially improved localization strategy. The resulting relaxed oversampling condition has a significant impact on the computational costs; in the offline phase as well as in the online phase, significant savings can be achieved.

Under a stability assumption on the method's basis, a rigorous wavenumber-explicit stability and error analysis of the proposed method was performed.

A sequence of numerical experiments demonstrated the effectiveness of the proposed multiscale method. In contrast to the LOD, also for relatively high wavenumbers, it yields faithful numerical approximations even for the rather small oversampling parameters $\ell = 2, 3$. We demonstrated that the proposed method can handle numerically challenging high-contrast heterogeneous Helmholtz problems. Furthermore, it was shown that the method is easily combined with perfectly matched layers (PML). We highlight that our approach may be transferred to other related problems, such as elastic wave propagation [11] and Maxwell's equations [28, 34], which have already been studied in the classical LOD setting.

REFERENCES

- [1] R. ALTMANN, P. HENNING, AND D. PETERSEIM, *Numerical homogenization beyond scale separation*, Acta Numer., 30 (2021), pp. 1–86, <https://doi.org/10.1017/S0962492921000015>.
- [2] I. M. BABUŠKA AND S. A. SAUTER, *Is the pollution effect of the FEM avoidable for the Helmholtz equation considering high wave numbers?*, SIAM J. Numer. Anal., 34 (1997), pp. 2392–2423, <https://doi.org/10.1137/S0036142994269186>.
- [3] D. BASKIN, E. A. SPENCE, AND J. WUNSCH, *Sharp high-frequency estimates for the Helmholtz equation and applications to boundary integral equations*, SIAM J. Math. Anal., 48 (2016), pp. 229–267, <https://doi.org/10.1137/15M102530X>.
- [4] M. BEBENDORF, *A note on the Poincaré inequality for convex domains*, Z. Anal. Anwend., 22 (2003), pp. 751–756, <https://doi.org/10.4171/ZAA/1170>.
- [5] J.-P. BERENGER, *A perfectly matched layer for the absorption of electromagnetic waves*, J. Comput. Phys., 114 (1994), pp. 185–200, <https://doi.org/10.1006/jcph.1994.1159>.

- [6] A. BERMÚDEZ, L. HERVELLA-NIETO, A. PRIETO, AND R. RODRÍGUEZ, *An optimal perfectly matched layer with unbounded absorbing function for time-harmonic acoustic scattering problems*, J. Comput. Phys., 223 (2007), pp. 469–488, <https://doi.org/10.1016/j.jcp.2006.09.018>.
- [7] T. BETCKE, S. N. CHANDLER-WILDE, I. G. GRAHAM, S. LANGDON, AND M. LINDNER, *Condition number estimates for combined potential integral operators in acoustics and their boundary element discretisation*, Numer. Methods Partial Differential Equations, 27 (2011), pp. 31–69, <https://doi.org/10.1002/num.20643>.
- [8] S. C. BRENNER, J. C. GARAY, AND L.-Y. SUNG, *Additive Schwarz preconditioners for a localized orthogonal decomposition method*, Electron. Trans. Numer. Anal., 54 (2021), pp. 234–255, https://doi.org/10.1553/etna_vol54s234.
- [9] S. C. BRENNER AND L. R. SCOTT, *The Mathematical Theory of Finite Element Methods*, 3rd ed., Texts in Applied Mathematics 15, Springer, New York, 2008, <https://doi.org/10.1007/978-0-387-75934-0>.
- [10] F. BREZZI AND M. FORTIN, *Mixed and Hybrid Finite Element Methods*, Springer Series in Computational Mathematics 15, Springer, 1991.
- [11] D. L. BROWN AND D. GALLISTL, *Multiscale sub-grid correction method for time-harmonic high-frequency elastodynamics with wave number explicit bounds*, Comput. Methods Appl. Math., 23 (2023), pp. 65–82, <https://doi.org/10.1515/cmam-2022-0041>.
- [12] D. L. BROWN, D. GALLISTL, AND D. PETERSEIM, *Multiscale Petrov-Galerkin method for high-frequency heterogeneous Helmholtz equations*, in Meshfree Methods for Partial Differential Equations VIII, Lect. Notes Comput. Sci. Eng. 115, Springer, Cham, 2017, pp. 85–115, https://doi.org/10.1007/978-3-319-51954-8_6.
- [13] A. BUHR AND K. SMETANA, *Randomized local model order reduction*, SIAM J. Sci. Comput., 40 (2018), pp. A2120–A2151, <https://doi.org/10.1137/17M1138480>.
- [14] T. CHAUMONT-FRELET, D. GALLISTL, S. NICAISE, AND J. TOMEZYK, *Wavenumber-explicit convergence analysis for finite element discretizations of time-harmonic wave propagation problems with perfectly matched layers*, Commun. Math. Sci., 20 (2022), pp. 1–52, <https://doi.org/10.4310/CMS.2022.v20.n1.a1>.
- [15] T. CHAUMONT-FRELET AND F. VALENTIN, *A multiscale hybrid-mixed method for the Helmholtz equation in heterogeneous domains*, SIAM J. Numer. Anal., 58 (2020), pp. 1029–1067, <https://doi.org/10.1137/19M1255616>.
- [16] Y. CHEN, T. Y. HOU, AND Y. WANG, *Exponentially convergent multiscale methods for 2D high frequency heterogeneous Helmholtz equations*, Multiscale Model. Simul., 21 (2023), pp. 849–883, <https://doi.org/10.1137/22M1507802>.
- [17] Y. K. CHEUNG, W. G. JIN, AND O. C. ZIENKIEWICZ, *Solution of Helmholtz equation by Trefftz method*, J. Numer. Methods Engng., 32 (1991), pp. 63–78, <https://doi.org/10.1002/nme.1620320105>.
- [18] M. CHUPENG, C. ALBER, AND R. SCHEICHL, *Wavenumber explicit convergence of a multiscale generalized finite element method for heterogeneous Helmholtz problems*, SIAM J. Numer. Anal., 61 (2023), pp. 1546–1584, <https://doi.org/10.1137/21M1466748>.
- [19] F. COLLINO AND C. TSOGKA, *Application of the perfectly matched absorbing layer model to the linear elastodynamic problem in anisotropic heterogeneous media*, Geophys., 66 (2001), pp. 294–307, <https://doi.org/10.1190/1.1444908>.
- [20] P. CUMMINGS AND X. FENG, *Sharp regularity coefficient estimates for complex-valued acoustic and elastic Helmholtz equations*, Math. Models Methods Appl. Sci., 16 (2006), pp. 139–160, <https://doi.org/10.1142/S021820250600108X>.
- [21] C. ENGWER, P. HENNING, A. MÅLQVIST, AND D. PETERSEIM, *Efficient implementation of the localized orthogonal decomposition method*, Comput. Methods Appl. Mech. Engng., 350 (2019), pp. 123–153, <https://doi.org/10.1016/j.cma.2019.02.040>.
- [22] A. ERN AND J.-L. GUERMOND, *Theory and Practice of Finite Elements*, Applied Mathematical Sciences 159, Springer-Verlag, New York, 2004, <https://doi.org/10.1007/978-1-4757-4355-5>.
- [23] S. ESTERHAZY AND J. M. MELENK, *On stability of discretizations of the Helmholtz equation*, in Numerical Analysis of Multiscale Problems, Lect. Notes Comput. Sci. Eng. 83, Springer, Heidelberg, 2012, pp. 285–324, https://doi.org/10.1007/978-3-642-22061-6_9.
- [24] P. FREESE, M. HAUCK, T. KEIL, AND D. PETERSEIM, *A super-localized generalized finite element method*, Numer. Math., 156 (2024), pp. 205–235, <https://doi.org/10.1007/s00211-023-01386-4>.
- [25] S. FU AND K. GAO, *A fast solver for the Helmholtz equation based on the generalized multiscale finite-element method*, Geophys. J. Int., 211 (2017), pp. 797–813, <https://doi.org/10.1093/gji/ggx343>.

- [26] S. FU, G. LI, R. CRASTER, AND S. GUENNEAU, *Wavelet-based edge multiscale finite element method for Helmholtz problems in perforated domains*, *Multiscale Model. Simul.*, 19 (2021), pp. 1684–1709, <https://doi.org/10.1137/19M1267180>.
- [27] J. GALKOWSKI, D. LAFONTAINE, AND E. A. SPENCE, *Local absorbing boundary conditions on fixed domains give order-one errors for high-frequency waves*, *IMA J. Numer. Anal.*, (2023), drad058, <https://doi.org/10.1093/imanum/drad058>.
- [28] D. GALLISTL, P. HENNING, AND B. VERFÜRTH, *Numerical homogenization of $\mathbf{H}(\text{curl})$ -problems*, *SIAM J. Numer. Anal.*, 56 (2018), pp. 1570–1596, <https://doi.org/10.1137/17M1133932>.
- [29] D. GALLISTL AND D. PETERSEIM, *Stable multiscale Petrov-Galerkin finite element method for high frequency acoustic scattering*, *Comput. Methods Appl. Mech. Engrg.*, 295 (2015), pp. 1–17, <https://doi.org/10.1016/j.cma.2015.06.017>.
- [30] I. G. GRAHAM, O. R. PEMBERY, AND E. A. SPENCE, *The Helmholtz equation in heterogeneous media: A priori bounds, well-posedness, and resonances*, *J. Differential Equations*, 266 (2019), pp. 2869–2923, <https://doi.org/10.1016/j.jde.2018.08.048>.
- [31] I. G. GRAHAM AND S. A. SAUTER, *Stability and finite element error analysis for the Helmholtz equation with variable coefficients*, *Math. Comp.*, 89 (2020), pp. 105–138, <https://doi.org/10.1090/mcom/3457>.
- [32] M. HAUCK AND D. PETERSEIM, *Multi-resolution localized orthogonal decomposition for Helmholtz problems*, *Multiscale Model. Simul.*, 20 (2022), pp. 657–684, <https://doi.org/10.1137/21M1414607>.
- [33] M. HAUCK AND D. PETERSEIM, *Super-localization of elliptic multiscale problems*, *Math. Comp.*, 92 (2023), pp. 981–1003, <https://doi.org/10.1090/mcom/3798>.
- [34] P. HENNING AND A. PERSSON, *Computational homogenization of time-harmonic Maxwell's equations*, *SIAM J. Sci. Comput.*, 42 (2020), pp. B581–B607, <https://doi.org/10.1137/19M1293818>.
- [35] P. HENNING AND D. PETERSEIM, *Oversampling for the multiscale finite element method*, *Multiscale Model. Simul.*, 11 (2013), pp. 1149–1175, <https://doi.org/10.1137/120900332>.
- [36] R. HIPTMAIR, A. MOIOLA, AND I. PERUGIA, *A Survey of Trefftz Methods for the Helmholtz Equation*, *Lect. Notes Comput. Sci. Eng.* 114, Springer, 2016, pp. 237–278.
- [37] R. KORNHUBER, D. PETERSEIM, AND H. YSERENTANT, *An analysis of a class of variational multiscale methods based on subspace decomposition*, *Math. Comp.*, 87 (2018), pp. 2765–2774, <https://doi.org/10.1090/mcom/3302>.
- [38] R. KORNHUBER AND H. YSERENTANT, *Numerical homogenization of elliptic multiscale problems by subspace decomposition*, *Multiscale Model. Simul.*, 14 (2016), pp. 1017–1036, <https://doi.org/10.1137/15M1028510>.
- [39] J.-L. LIONS AND E. MAGENES, *Non-homogeneous Boundary Value Problems and Applications*, Vol. I, *Die Grundlehren der mathematischen Wissenschaften* 181, Springer-Verlag, New York-Heidelberg, 1972.
- [40] A. MÅLQVIST AND D. PETERSEIM, *Localization of elliptic multiscale problems*, *Math. Comp.*, 83 (2014), pp. 2583–2603, <https://doi.org/10.1090/S0025-5718-2014-02868-8>.
- [41] A. MÅLQVIST AND D. PETERSEIM, *Numerical Homogenization by Localized Orthogonal Decomposition*, *SIAM Spotlights* 5, SIAM, Philadelphia, 2021, <https://doi.org/10.1137/1.9781611976458>.
- [42] J. M. MELENK, *On Generalized Finite-Element Methods*, Ph.D. thesis, University of Maryland, College Park, 1995.
- [43] J. M. MELENK, A. PARSANIA, AND S. SAUTER, *General DG-methods for highly indefinite Helmholtz problems*, *J. Sci. Comput.*, 57 (2013), pp. 536–581, <https://doi.org/10.1007/s10915-013-9726-8>.
- [44] J. M. MELENK AND S. SAUTER, *Convergence analysis for finite element discretizations of the Helmholtz equation with Dirichlet-to-Neumann boundary conditions*, *Math. Comp.*, 79 (2010), pp. 1871–1914, <https://doi.org/10.1090/S0025-5718-10-02362-8>.
- [45] J. M. MELENK AND S. SAUTER, *Wavenumber explicit convergence analysis for Galerkin discretizations of the Helmholtz equation*, *SIAM J. Numer. Anal.*, 49 (2011), pp. 1210–1243, <https://doi.org/10.1137/090776202>.
- [46] A. MOIOLA AND E. A. SPENCE, *Is the Helmholtz equation really sign-indefinite?*, *SIAM Rev.*, 56 (2014), pp. 274–312, <https://doi.org/10.1137/120901301>.
- [47] M. OHLBERGER AND B. VERFÜRTH, *A new heterogeneous multiscale method for the Helmholtz equation with high contrast*, *Multiscale Model. Simul.*, 16 (2018), pp. 385–411, <https://doi.org/10.1137/16M1108820>.
- [48] L. E. PAYNE AND H. F. WEINBERGER, *An optimal Poincaré inequality for convex domains*, *Arch. Ration. Mech. Anal.*, 5 (1960), pp. 286–292, <https://doi.org/10.1007/BF00252910>.

- [49] D. PETERSEIM, *Variational multiscale stabilization and the exponential decay of fine-scale correctors*, in Building Bridges: Connections and Challenges in Modern Approaches to Numerical Partial Differential Equations, Lect. Notes Comput. Sci. Eng. 114, Springer, 2016, pp. 341–367.
- [50] D. PETERSEIM, *Eliminating the pollution effect in Helmholtz problems by local subscale correction*, Math. Comp., 86 (2017), pp. 1005–1036, <https://doi.org/10.1090/mcom/3156>.
- [51] D. PETERSEIM AND B. VERFÜRTH, *Computational high frequency scattering from high-contrast heterogeneous media*, Math. Comp., 89 (2020), pp. 2649–2674, <https://doi.org/10.1090/mcom/3529>.
- [52] T. ROUBÍČEK, *Nonlinear Partial Differential Equations with Applications*, 2nd ed., International Series of Numerical Mathematics 153, Birkhäuser/Springer Basel AG, Basel, 2013, <https://doi.org/10.1007/978-3-0348-0513-1>.
- [53] S. SAUTER AND C. TORRES, *Stability estimate for the Helmholtz equation with rapidly jumping coefficients*, Z. Angew. Math. Phys., 69 (2018), 139, <https://doi.org/10.1007/s00033-018-1031-9>.
- [54] E. A. SPENCE, *Wavenumber-explicit bounds in time-harmonic acoustic scattering*, SIAM J. Math. Anal., 46 (2014), pp. 2987–3024, <https://doi.org/10.1137/130932855>.
- [55] M. G. STOJEK, *Least-squares Trefftz-type elements for the Helmholtz equation*, Internat. J. Numer. Methods Engrg., 41 (1998), pp. 831–849, [https://doi.org/10.1002/\(SICI\)1097-0207\(19980315\)41:5<831::AID-NME311>3.0.CO;2-V](https://doi.org/10.1002/(SICI)1097-0207(19980315)41:5<831::AID-NME311>3.0.CO;2-V).
- [56] A. TOSELLI AND O. WIDLUND, *Domain Decomposition Methods—Algorithms and Theory*, Springer Series in Computational Mathematics 34, Springer-Verlag, Berlin, 2005, <https://doi.org/10.1007/b137868>.
- [57] E. TREFFTZ, *Ein Gegenstück zum Ritzschen Verfahren*, Verhandlungen des II, Kongress für technische Mechanik, Zürich, (1926), pp. 131–137.
- [58] R. VERFÜRTH, *A Review of A Posteriori Error Estimation and Adaptive Mesh-Refinement Techniques*, Wiley-Teubner, New York, 1996.